Department of the Navy
Bureau of Ordnance
Contract NOrd-16200
Task 1

CAVITY SHAPES FOR CIRCULAR DISKS AT ANGLES OF ATTACK

R. L. Waid

Hydrodynamics Laboratory
CALIFORNIA INSTITUTE OF TECHNOLOGY
Pasadena, California

Report No. E-73.4 September 1957

Department of the Navy
Bureau of Ordnance
Contract NOrd-16200
Task 1

CAVITY SHAPES FOR CIRCULAR DISKS AT ANGLES OF ATTACK

R. L. Waid

Reproduction in whole or in part is permitted for any purpose
of the United States Government

Hydrodynamics Laboratory
California Institute of Technology
Pasadena, California

Report No. E - 73.4

September 1957

C O N T E N T S

ABSTRACT

The shape of the cavity formed in water by a circular disk at an angle of attack is derived. The empirical evaluation is based on experimental data obtained with air cavities in the Free Surface Water Tunnel. The effects of model size, free stream velocity and cavitation number on cavity shape are presented.

The profile shape of the cavity is assumed to be composed of two superposable phenomena:

(1) the cavity shape without gravity effects

(2) the displacement of the cavity due to gravity

An empirical relation is obtained for the buoyant displacement of the cavity centerline. A quasi-elliptical equation is derived which accurately describes the shape of the cavity about its centerline for the disk at zero angle of attack. The equation is modified and applied to the profile shape of a cavity formed by a circular disk at angles of attack up to 30 degrees. All experimental data are presented in both graphic and analytic form.

I. INTRODUCTION

The shape of the cavity formed by a flat disk in a moving fluid has been studied experimentally by a number of investigators.[1,2,3*] These previous studies describe the characteristic dimensions (half length and maximum diameter) of the cavities formed by disks at zero attack angle where the flat face of the disk is normal to the flow direction. Eisenberg[4] describes an empirical representation of the shape of such a cavity for one specific set of test conditions. This report presents the results of an experimental program which was conducted for the purpose of empirically describing the shape of a flat disk cavity for a variety of conditions. The experimental program was performed in the Free Surface Water Tunnel[5] of the Hydrodynamics Laboratory using air-sustained cavities.[6, 7] The experimental variables which were considered were the disk diameter, angle of attack, free stream velocity, and cavitation number.

For the purposes of this study, the observed profile shape of a cavity is assumed to be composed of two separate but superposable phenomena. One is the buoyant effect of gravity on the cavity and the other is the shape of the cavity formed in the absence of buoyant effects. The empirical analysis treats these two phenomena separately; however the actual cavity profile may be obtained by simply superimposing the cavity shape without buoyant effects upon a centerline which is displaced because of buoyancy.

One section of this report describes the effect of model size, free stream velocity, and cavitation number on the buoyant displacement of the cavity centerline. A second section describes the shape of cavities formed at zero attack angle for various disk sizes, free stream velocities and cavitation numbers. A third section describes the profile shape of cavities formed by a flat disk for various attack angles and cavitation numbers. The latter two sections describe the shape of a flat disk cavity by a practical empirical representation. This representation is derived solely for the first half length of the cavity between the disk and the point of the maximum radius of the cavity. However, a symmetrical application of the derived

---

* Superscripts refer to references in bibliography.

cavity shape is a reasonable approximation in the region downstream of the maximum radius.

A calibration of the rise of the free surface of the moving water in the test section was performed as an essential part of this program, and the results are presented in the appendix of this report.

The forces and moments on a pitched disk in full cavity flow are presented in a Hydrodynamics Laboratory report by Kiceniuk.[8]

II. MODEL INSTALLATION

The models for this experimental program were 1/2, 3/4 and 1-inch diameter circular flat disks, as shown in Fig. 1.

The models were mounted on a 1-inch diameter sting which was attached at the lower end of a surface-piercing strut, Fig. 2. An internal duct passing through the strut and the sting provided the air supply for the maintenance of the air cavity. A small tube was attached along the side of the strut and the sting to allow the pressure in the cavity to be measured. The vibration of the sting and strut was found to be intolerable during the pitched disk tests, so a shorter sting configuration, Fig. 3, was used for that phase of the program.

The model was placed in the center of the width and twelve inches above the bottom of the twenty-by-twenty-inch water tunnel test section. The model was pitched in a vertical plane to provide the variation of attack angle.

III. EXPERIMENTAL PROCEDURES

The method of obtaining the experimental conditions was to first set the model size, angle of attack and free stream velocity, and then vary the air flow into the cavity from maximum to minimum to establish the limits for which a stable cavity could be maintained. The airflow was then adjusted so that approximately five different cavity pressures could be obtained within this range.

Since the depth of the disk was fixed, the changes of the cavity pressure provided the desired variations in the cavitation number. The cavitation number (σ) is defined as

$$\sigma = \frac{P_o - P_k}{\rho/2\ V^2}$$

where P_o = Static pressure at the centerline of the disk

P_k = Pressure of gas in cavity

ρ = Density of water at test conditions

V = Velocity of water in the free stream

The profile shape of the cavity was photographed for each set of stable test conditions. The exposure of one-fiftieth of a second provided a sufficiently long time average of the cavity shape without impairing the clarity of the cavity profile. Figure 4 is a typical example of the data photographs. The light background makes the cavity profile stand out in silhouette. The dark framing above and below the cavity reduced the reflected light from the upper and lower edges of the cavity, thereby increasing the definition of the cavity profile. The dark stripe in the background is a horizontal line used as a reference for the photographs.

The cavity shapes were measured by projecting the photographic negatives and measuring the position of the upper and lower edges of the cavity relative t the horizontal reference stripe. These measurements were obtained at various axial positions from the edge of the disk to a point well beyond the maximum diameter of the cavity. The estimated accuracy of the measurements was $\pm$ 0.015 inches relative to the model scale.

The variable test conditions for the disk at zero attack angle were:

a. disk diameter (1/2, 3/4, 1 inch)
b. free stream velocity (12, 16, 20, 24 fps)
c. cavitation number (0.035 to 0.172 depending upon model size and free stream velocity).

The 1-inch diameter disk was tested at 24 fps for variable:

a. angle of attack (-30, -20, +10, +20 and +30 degrees)
b. cavitation number (0.043 to 0.098 depending upon angle of attack).

The free surface of the water rises slightly along the working section. Since the surface rise varies with the free stream velocity, it was necessary to calibrate the surface profile and to take this rise into account when comparing cavity profiles at various free stream velocities. The procedure and results of this portion of the tests are presented in Appendix I.

IV. EXPERIMENTAL RESULTS

A. Buoyant Displacement of Cavity

The effect of gravity on the cavity shape in low velocity is evident by the buoyant displacement of the gas-filled cavity, Fig. 5. Visual observation of the cavities indicates that there is no significant gravitational distortion of the circular cross section of the cavity for its first half length. Downstream of the maximum radius obvious distortion appears as the bottom of the cavity rises inside the circular section and eventually separates the cavity into either a twin vortex or a deformed re-entrant jet. The photographs of the experimental cavities at zero attack angle were measured to obtain the vertical displacement of the cavity centerline which is defined as midway between the upper and lower profile edges of the cavity. This definition has practical significance over the forward half length of the cavity where the cross section is generally circular. Since the cavity displacements were measured from a horizontal reference, the data were corrected for the rise of the free water surface.

Figure 6 shows the corrected cavity centerline rise for a 1-inch diameter disk at 24 fps. Variation of cavitation number does not appear to have an appreciable effect upon the centerline displacement. Figure 7 shows the centerline rise at 24 fps for all data with the 1/2, 3/4 and 1-inch diameter disks. The curves indicate that there is no significant size effect on the centerline displacement. Figure 8 presents the average centerline rise for each diameter disk for the four free stream velocities tested. It is apparent that the effect of velocity is very pronounced and systematic. Figure 9, a replot of Fig. 8 on a log-log scale, emphasized this systematic behavior. Figure 10 shows these centerline displacements plotted as a function of time, i.e., the distance along the centerline divided by the free stream velocity. Since the displacement curves as a function of time form a common line, Fig. 10, the following empirical equation is used to describe

the centerline rise due to buoyancy:

$$CLR = 163.3\ t^2 \tag{2}$$

where CLR = centerline rise due to buoyancy (inches)

$t = \frac{x}{v}$ = time (seconds), and

x = distance from disk

v = free stream velocity

This result is in approximate agreement with that which would be obtained by assuming a coefficient of virtual mass caused by the buoyant acceleration of the cavity and by considering a drag force due to the buoyant velocity of the cavity.

Therefore, it can be concluded that within the range of variables, as reported herein, the buoyant displacement of the cavity centerline is

1. independent of the size of the disk,
2. independent of the cavitation number, and
3. dependent solely on the time for flow past the cavity as detailed in the above equation.

B. Cavity Shape at Zero Attack Angle

This section describes an empirical representation of the shape of the first half length of a cavity from which buoyant effects have been removed. Figure 11 presents the analytic description of a circular disk cavity as considered in this section. The x-y coordinate system originates at the center of the flat face of the disk with the x-axis parallel to the flow direction. The commonly used characteristic dimensions of the cavity, half length and maximum diameter, are denoted a_o and d_m, respectively.

The analytic equation describing the cavity profile must meet the requirements of being tangent to the disk surface at the point of flow separation and parallel to the free stream direction at the point of maximum diameter. To satisfy these requirements, the analytic cavity shape was assumed to be of the quasi-elliptical form

$$\left(\frac{y - y_o}{b_o}\right)^n + \left(\frac{x - a_o}{a_o}\right)^2 = 1 \tag{3}$$

where y = radial distance to cavity at any axial position

x = axial distance from the center of the face of the circular disk

y_o = radial distance to the point of flow separation

b_o = radial distance from flow separation to maximum cavity diameter ($b_o = d_m/2 - y_o$)

a_o = axial distance from flow separation to point of maximum cavity diameter (a_o = half length)

n = empirical exponent

The cavity shape data at zero attack angle were first analyzed for the characteristic dimensions of the elliptical form of the cavities a_o and b_o. Dimensionless forms of these results are presented in Figs. 12 and 13 as functions of cavitation number independent of both model size and free stream velocity. The data for a_o/d, Fig. 12, are well represented by the following functions of cavitation number,

$$\frac{a_o}{d} = \frac{0.540}{\sigma^{1.118}} \qquad .035 \leq \sigma \leq .171 \tag{4}$$

Similarly the data for b_o/d, Fig. 13, are represented by a function of cavitation number,

$$\frac{b_o}{d} = \frac{0.267}{\sigma^{.568}} \qquad .035 \leq \sigma \leq .171 \tag{5}$$

Experimental data from Reichardt[1] have been included in Figs. 12 and 13 for comparison.

Secondly the cavity shape data were analyzed by a least squares method to determine values of n for equation (3). The cavity shapes were fitted by curves of the forms of equation (3) with b_o and y_o established from the experiments and with a_o and n as the variables. This produced values of the cavity half length (denoted a_o'/d for least squares method) Fig. 14, which are similar to but more scattered than the a_o/d data obtained from the experiments. The computed values of n, as shown in

Fig. 15, appear to be independent of the cavitation number with a numerical average of $n = 1.800$.

For convenience in computing the coordinates of the cavity profile, equation (3) can be solved for y as follows:

$$y = y_o + b_o \left[1 - \left(\frac{x}{a_o} - 1\right)^2\right]^{\frac{1}{n}} = y_o + b_o \phi. \qquad (6)$$

Values of ϕ for $n = 1.800$ are shown in Fig. 16 as functions of x/a_o. Cavity profile shapes can thus be computed by using equation (6) and Fig. 16, plus the characteristic dimensions from equations (4), (5) or Figs. 12, 13.

A check of the validity of the assumed cavity shape is shown in Fig. 17 where the difference between several measured cavity shapes and their corresponding computed cavity shapes are shown. The differences are in general less than the estimated reading accuracy for the measured cavity profile data. Hence the assumed quasi-elliptical cavity shape equation does accurately describe the shape of the cavity.

The following conclusions are drawn about the shape of a cavity formed by a circular disk at zero attack angle neglecting buoyancy:

1. The shape is independent of free stream velocity for a given cavitation number.
2. The size of the cavity is directly proportional to the disk diameter for a given cavitation number.
3. The proportions of the cavity are solely dependent upon the cavitation number, Figs. 12 and 13, and equations (4) and (5)
4. The shape of the cavity is accurately described by equation (3) and its more useful form, equation (6).

C. Cavity Profile Shape at Angles of Attack up to 30 Degrees

This section describes an empirical representation for the profile shape of the first half length of a cavity formed by a circular disk at an angle of attack relative to the free stream velocity. The effects of buoyancy have been removed from the analysis. The method of deriving the empirical cavity shape is to employ a generalized version of the equations presented for a disk at zero attack angle and to apply them using two simplifying approximations. The analytic results are implemented by experi-

mental data obtained with the 1-inch diameter disk as tested at 24 fps free stream velocity for pitch angles up to 30 degrees.

Fig.18 presents the generalized version of Fig.11 as it applies to the analytic description of a circular disk cavity at an angle of attack. Because of experimental difficulties caused by the supporting strut when using the short boom, only the lower profile edge of the cavity could be measured. Since the disk is pitched to both positive and negative angles, however, it is possible to ascertain the profile shape of both sides of the cavity at any attack angle by appropriate application of the available experimental results. For this purpose the experimental data presented in this section are not identified with positive or negative attack angles, but rather they are identified as belonging with either the cavity wall which separates from the farthest forward edge of the disk or the cavity wall which separates from the farthest downstream edge of the disk, Fig.18.

An examination of equation (3) shows that it can be applied to the case of the pitched disk in the following modified form:

$$\left(\frac{y - y_o}{b_o}\right)^n + \left(\frac{x - x_o - a_o}{a_o}\right)^2 = 1 \qquad (7)$$

where all terms are as defined for equation (3) with the additional term, x_o, being the axial distance from the center of the disk to the point of flow separation. Note that in this case $y_o = d/2 \cos \alpha$ and $x_o = d/2 \sin \alpha$. It is assumed that although the quasi-elliptical cavity shape is not tangent to the disk surface at the point of flow separation, as is the actual cavity, that there is no effect on the cavity shape beyond the immediate region of flow separation. Secondly, it is assumed that the value of $n = 1.800$ is applicable to the pitched disk case since the experimental values of n are within the scatter of the more numerous data for the disk at zero angle of attack.

In addition to these two assumptions, the values of a_o and b_o for both surfaces must be obtained before equation (7) can be employed to obtain the cavity profile. Figures 19 and 20 present the dimensionless experimental values of a_o/d and b_o/d as a function of cavitation number for angles of attack up to 30 degrees for both forward and downstream separation edges. Within the limited range of the experimental cavitation numbers,

a_o/d and b_o/d can be represented analytically as follows:

$$\frac{a_o}{d} = \frac{M}{\sigma^{1.118}} \qquad 0.043 \leq \sigma \leq 0.098 \tag{8}$$

and

$$\frac{b_o}{d} = \frac{Q}{\sigma^{S}} \qquad 0.043 \leq \sigma \leq 0.098 \tag{9}$$

where M is an empirical function, Fig. 21,

Q and S are empirical functions, Fig. 22.

This completes the information required to compute the profile shape of the pitched disk cavity based on the quasi-elliptical representation of equation (7).

A check of the success of this simplified analysis is shown in Fig. 23 where several computed and measured cavity shapes are compared. These plots indicate that the discrepancies between the shapes are generally less than five percent of the disk radius.

Thus the following conclusions are drawn for the case of the cavity profile formed by a pitched circular disk with buoyant effects removed:

1. The proportions of both forward and downstream separation edges of the profile are functions of both the cavitation number and the angle of attack of the disk, Figs. 19 - 22 and equations (8) and (9).

2. The shape of the cavity is satisfactorily described by equation (7) which is a slightly modified version of the equation for the zero angle of attack case, equation (3).

APPENDIX I

CALIBRATION OF THE FREE WATER SURFACE

The surface of the water in the Free Surface Water Tunnel is displaced from the horizontal by the boundary layer built up along the side and bottom walls of the tunnel and by the upstream influence of the diffuser back pressure. There has been no calibration of this surface displacement since a new surface skimmer was installed in the tunnel. For an accurate analysis of the centerline rise of air-sustained cavities, as presented in this report, it was necessary to know the surface displacement as a function of the free stream velocity.

The surface calibration was conducted photographically. This was done to avoid the errors inherent in the time consuming and inconsistent pointer method. Figure 24 shows the technique employed to obtain instantaneous measurements of a major portion of the free surface in the test section. A light was projected obliquely toward the underside of the water surface through the side-wall windows. A carefully levelled stripe was attached to the outside of the window several inches below the mean water level. A camera positioned on the opposite side of the test section photographed the image of the light source and the stripe as reflected from the slightly rippled surface of the flowing water. Three light sources were placed along the test section to high light the major testing regions. A typical photograph of the underside of the water surface by this technique is shown in Fig. 25. The distance between the upper edge of the stripe and the lower edge of the reflection from the water surface can be calibrated to give the actual height of the surface above the level stripe.

The calibration of the stripe to image distance was performed by coating the surface of stationary water with likopodium and taking photographs of the level water surface at several measured water heights. The distance between the stripe and its image was used to calibrate the flow photographs.

The height of the free surface was obtained from these photographs and is shown in Fig. 26 as a function of the distance from the entrance to the test section for several free stream velocities.

LIST OF FIGURES

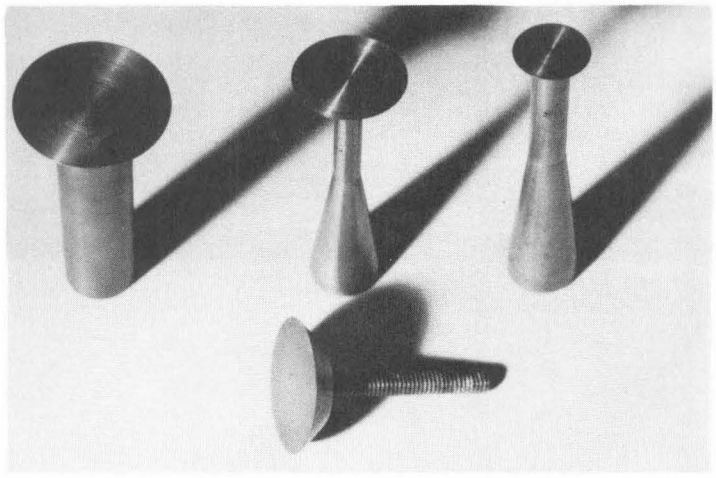

Fig. 1. Circular disk models

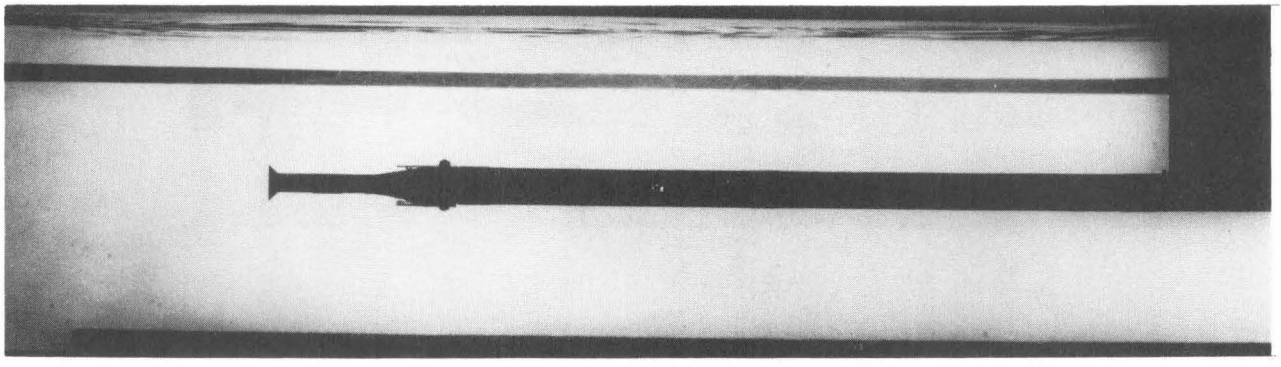

Fig. 2. Model installation on sting and strut

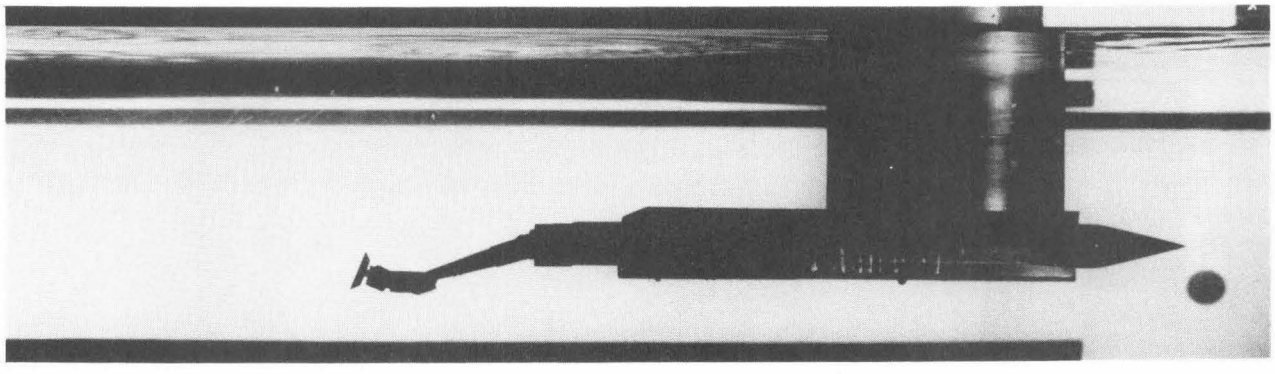

Fig. 3. Model installation on short sting and strut

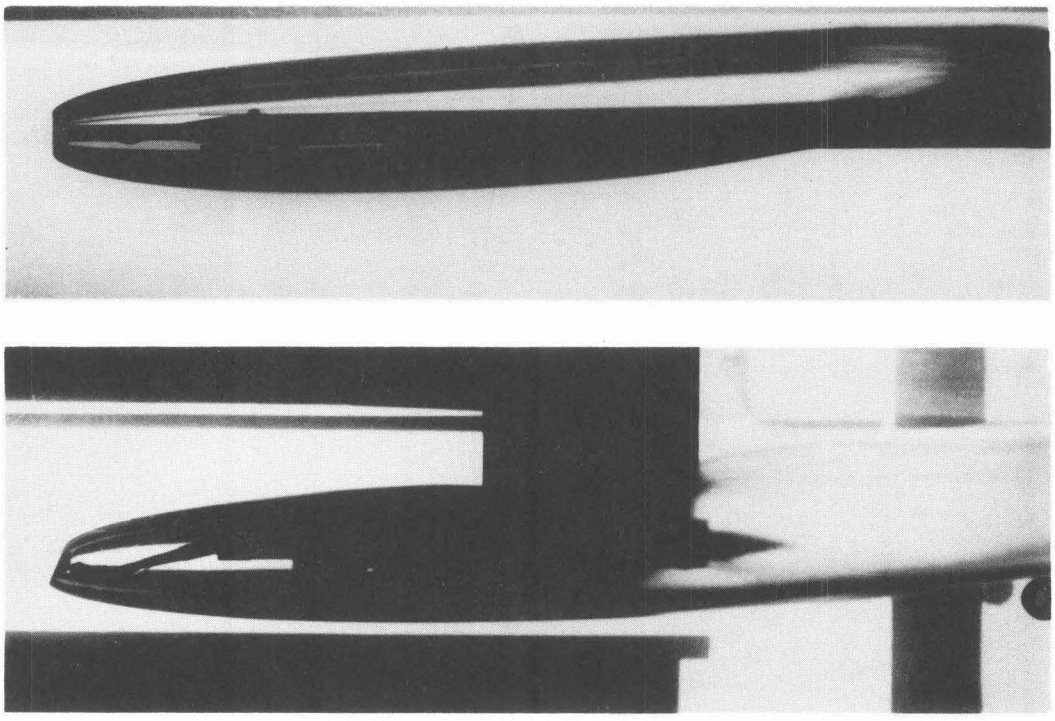

Fig. 4. Typical cavity profile photograph

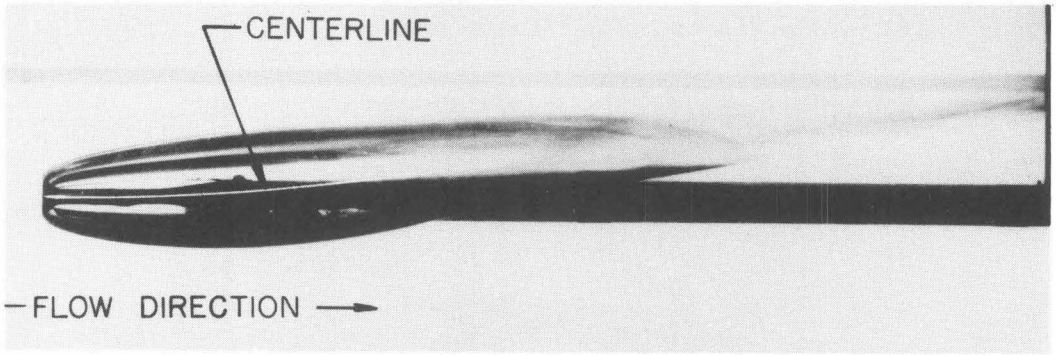

Fig. 5. Buoyant displacement of cavity

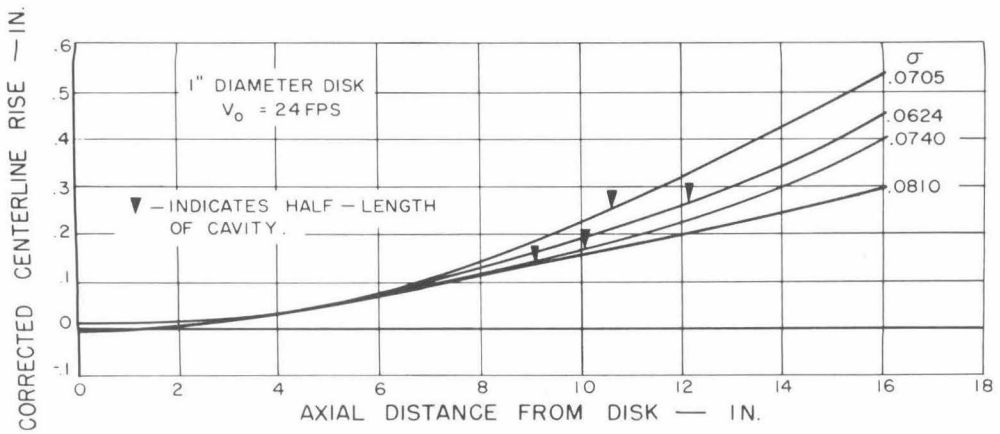

Fig. 6. Buoyant rise of centerline for 1-inch diameter disk at 24 fps

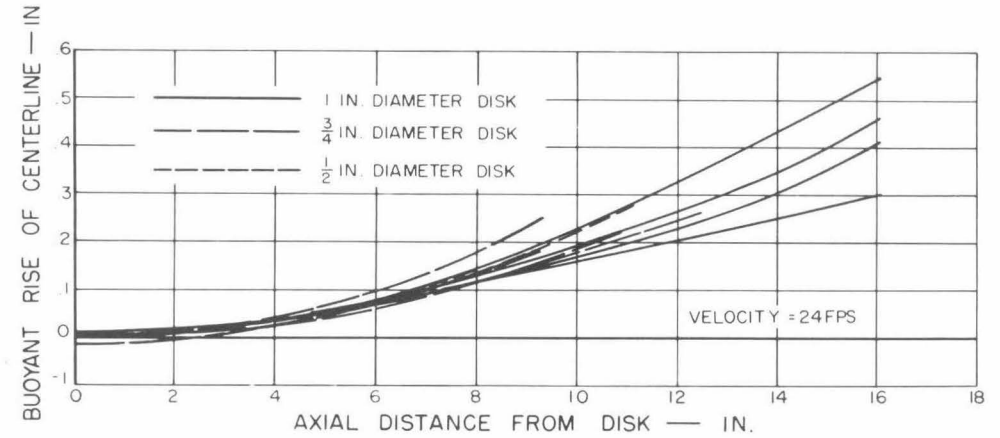

Fig. 7. Centerline rise for 1/2, 3/4 and 1-inch diameter disks at 24 fps

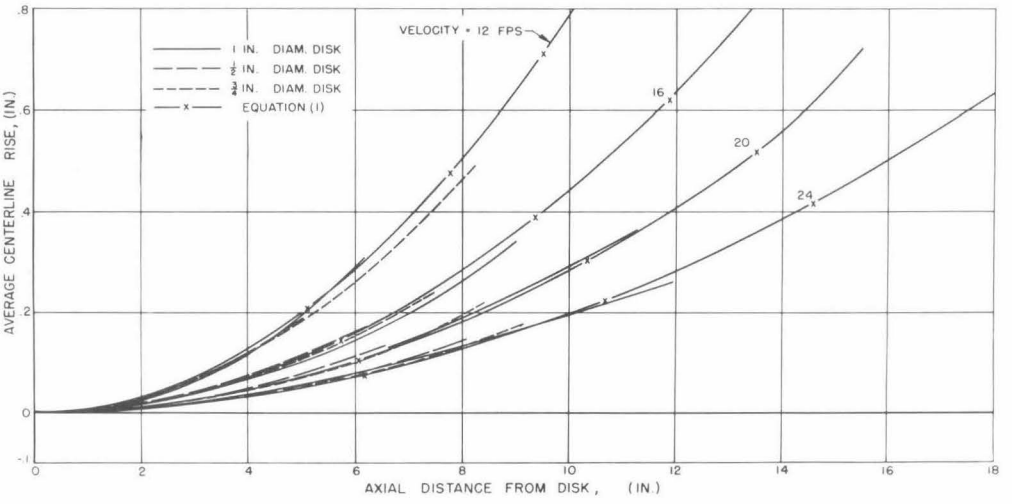

Fig. 8. Centerline rise for all diameter disks and all free stream velocities

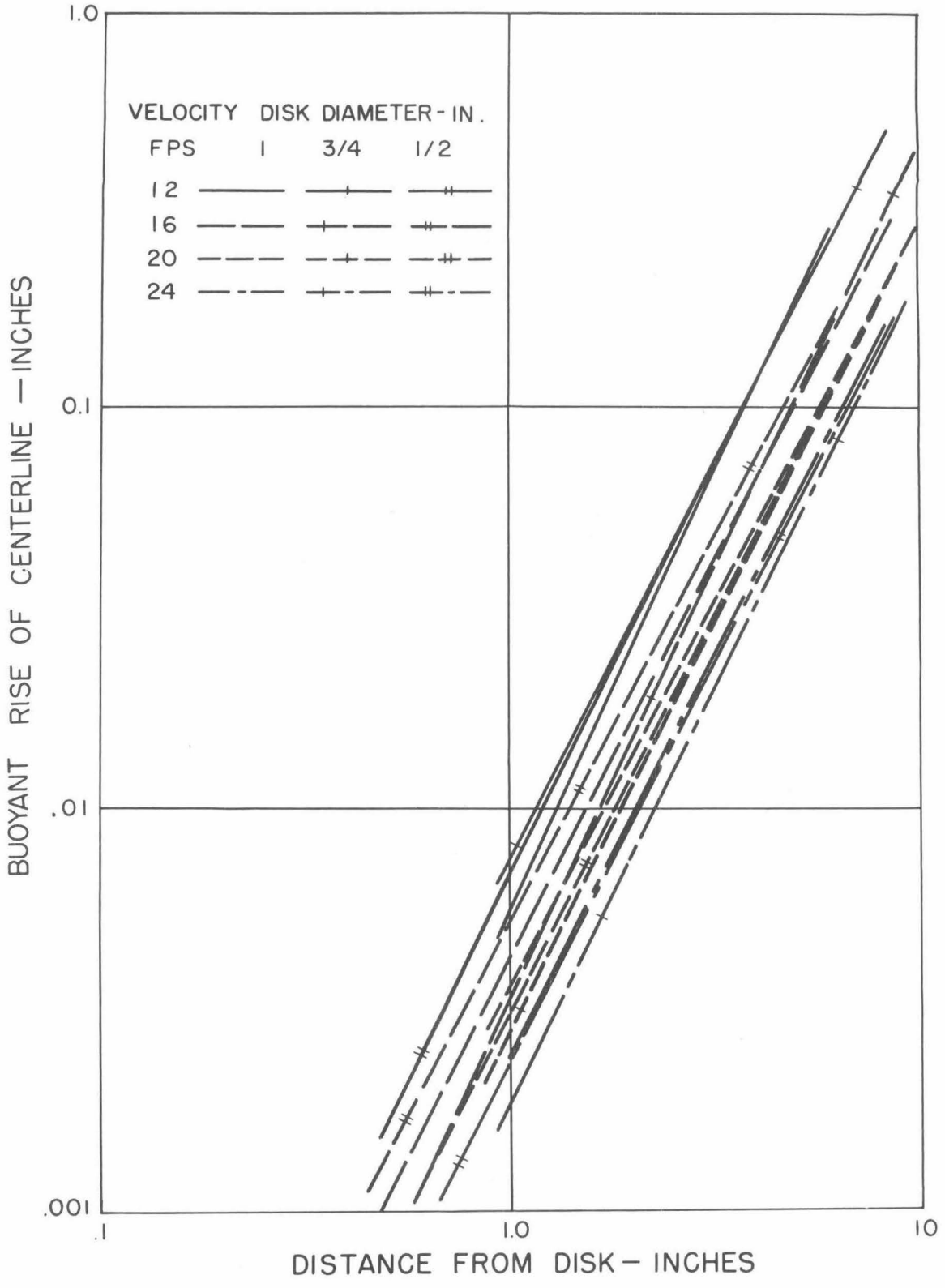

Fig. 9. Log-log plot of centerline rise as a function of distance

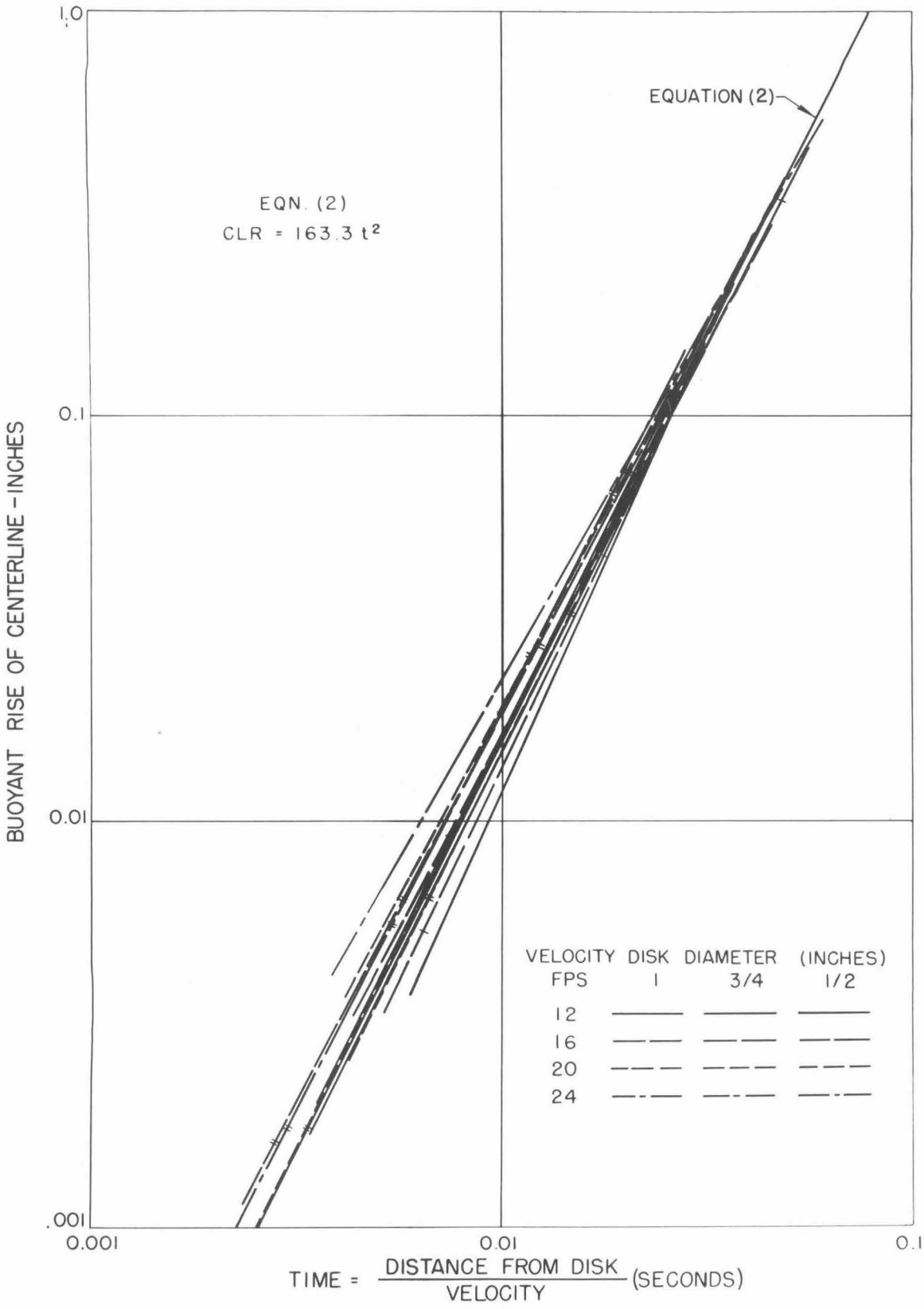

Fig. 10. Log-log plot of centerline rise as a function of time

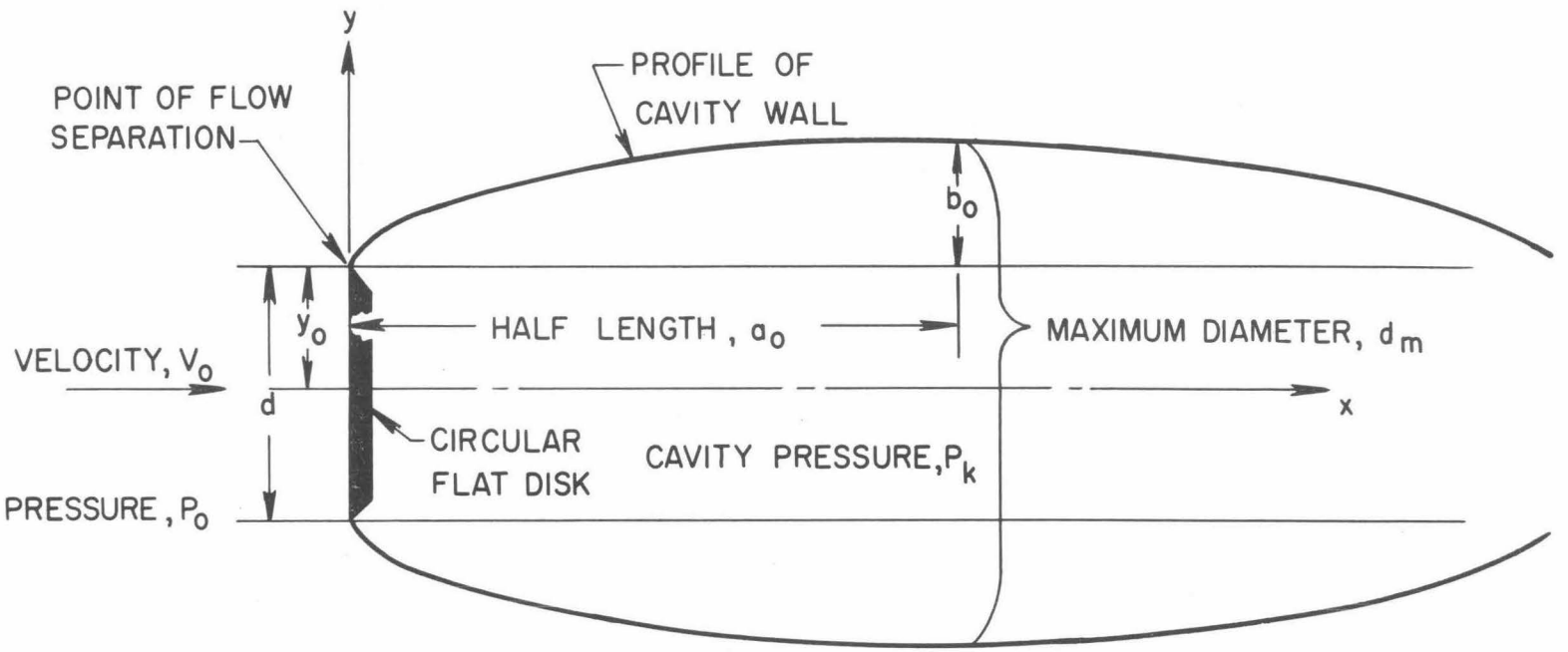

Fig. 11. Analytic description of circular disk cavity shape ($\alpha = 0^o$)

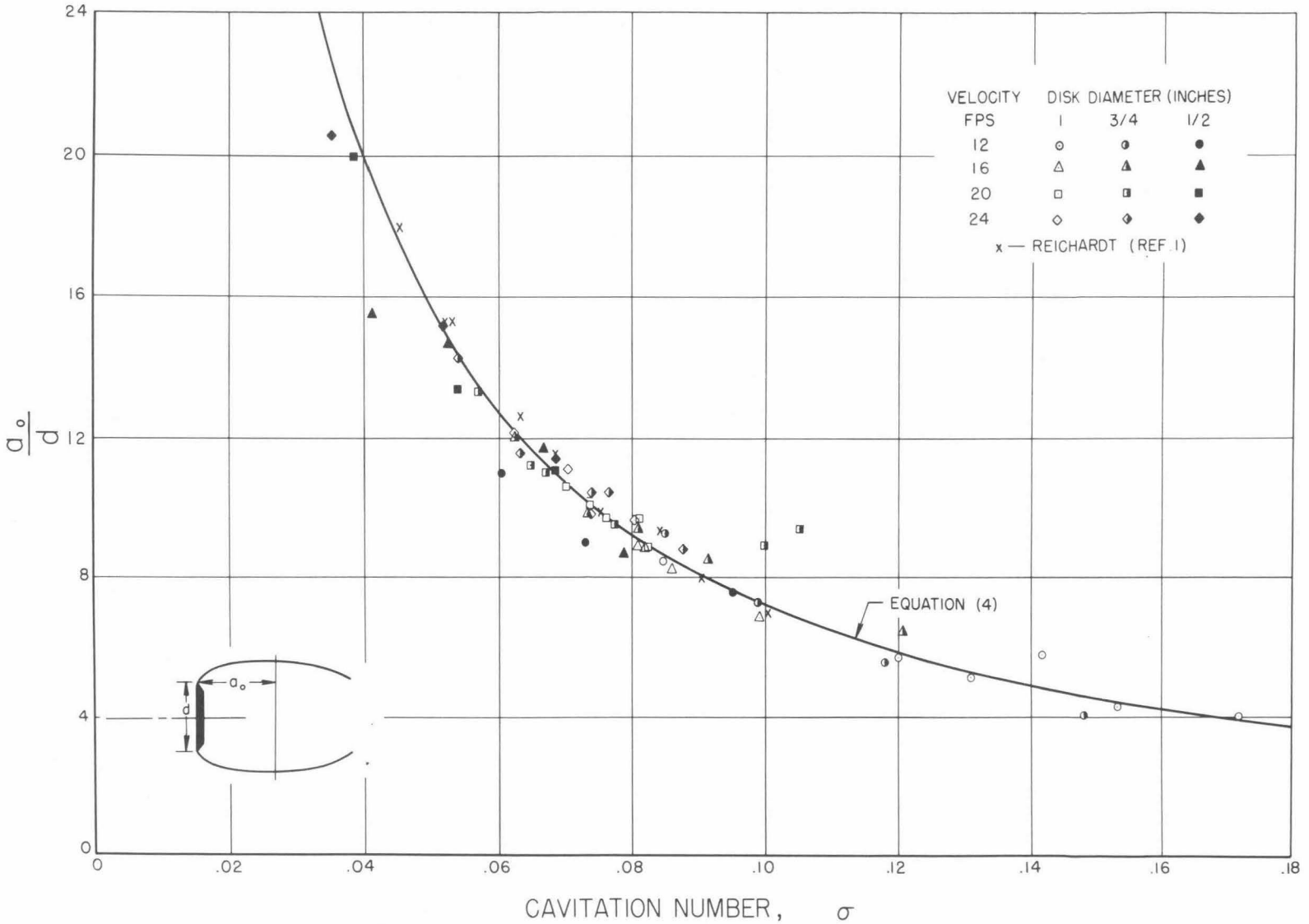

Fig. 12. Experimental half length, $\frac{a_o}{d}$, of circular disk cavities $(\alpha = 0^o)$

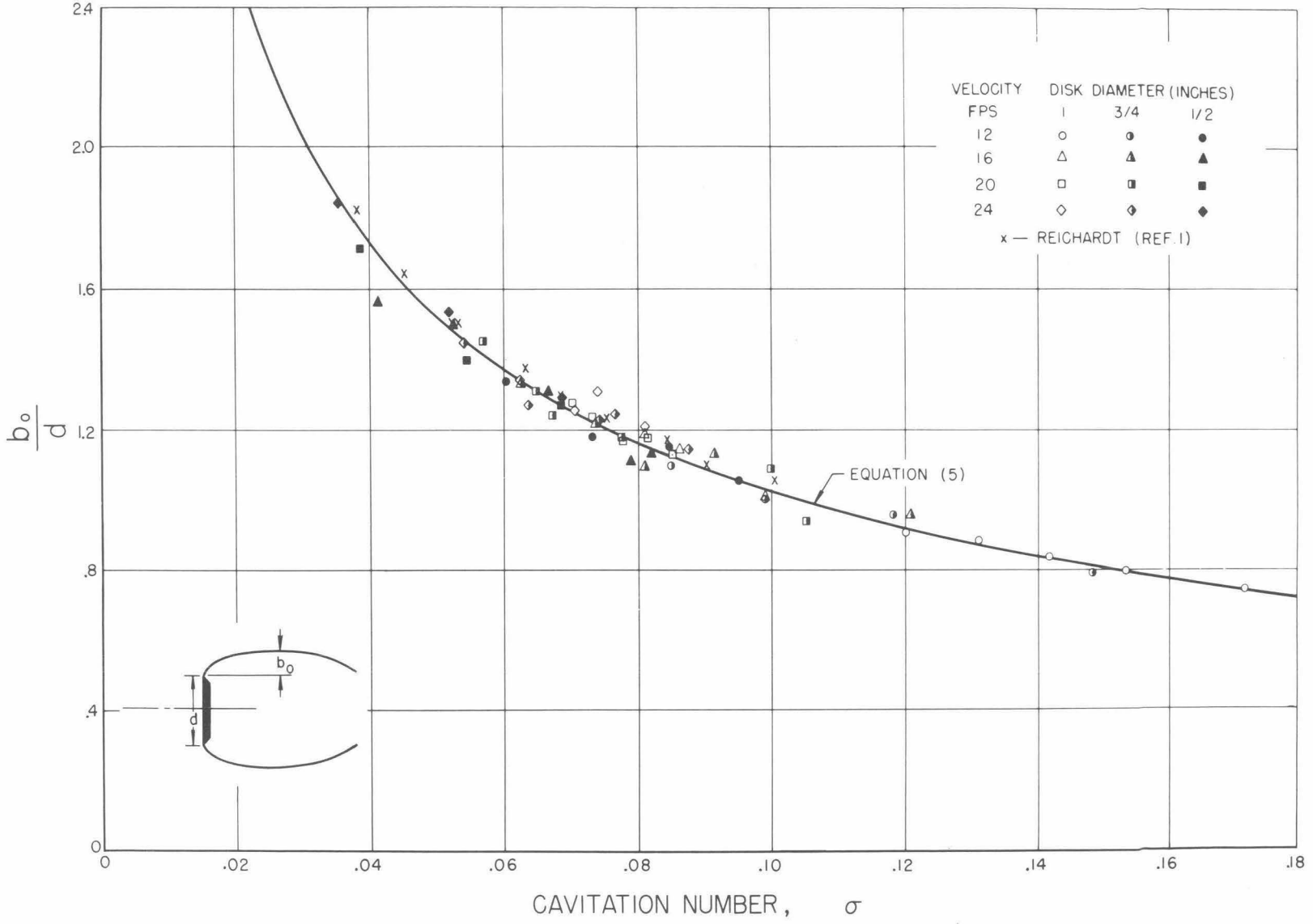

Fig. 13. Experimental $\frac{b_o}{d}$ of circular disk cavities $(\alpha = 0^o)$

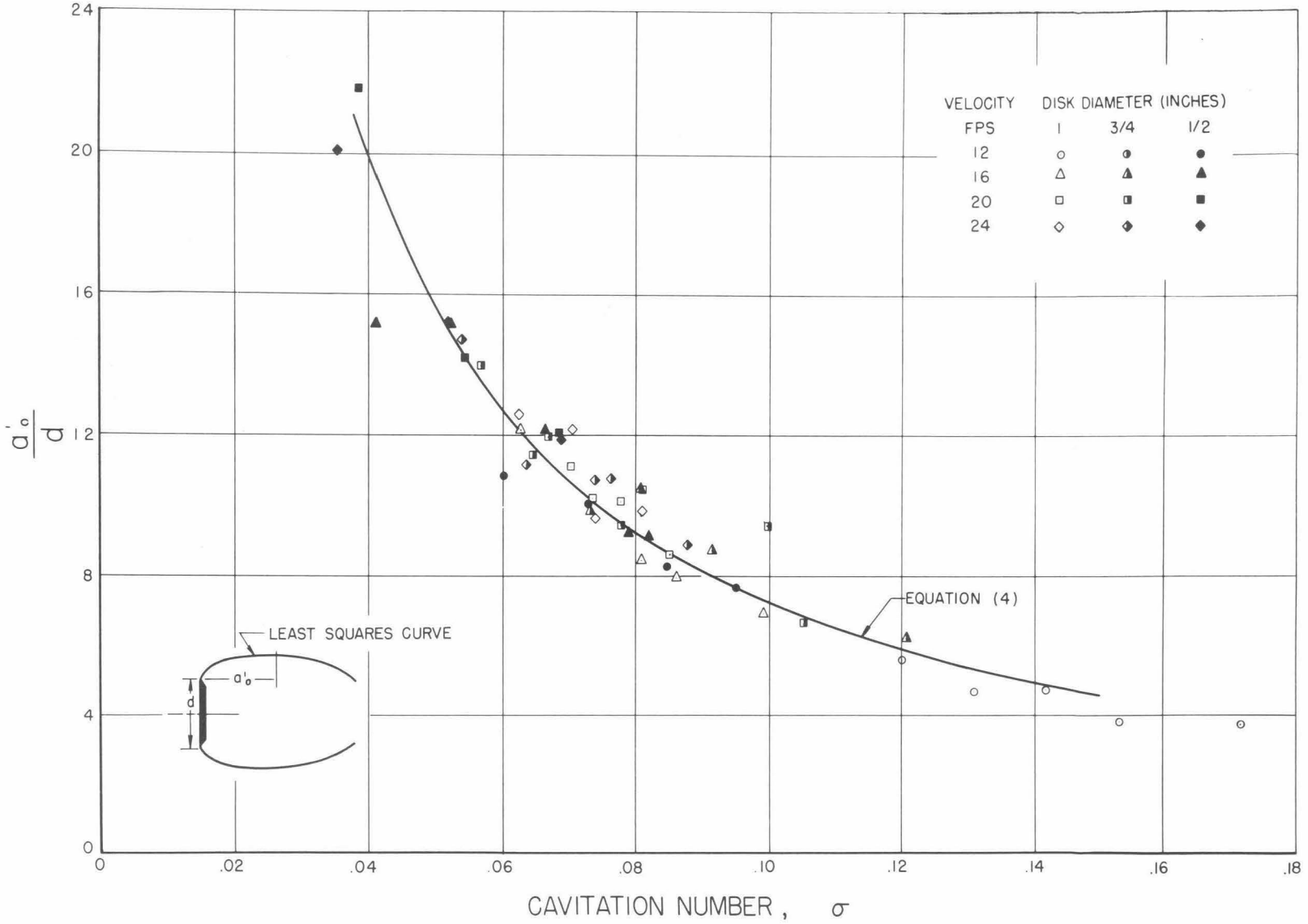

Fig. 14. a_o'/d as a function of cavitation number ($\alpha = 0^o$)

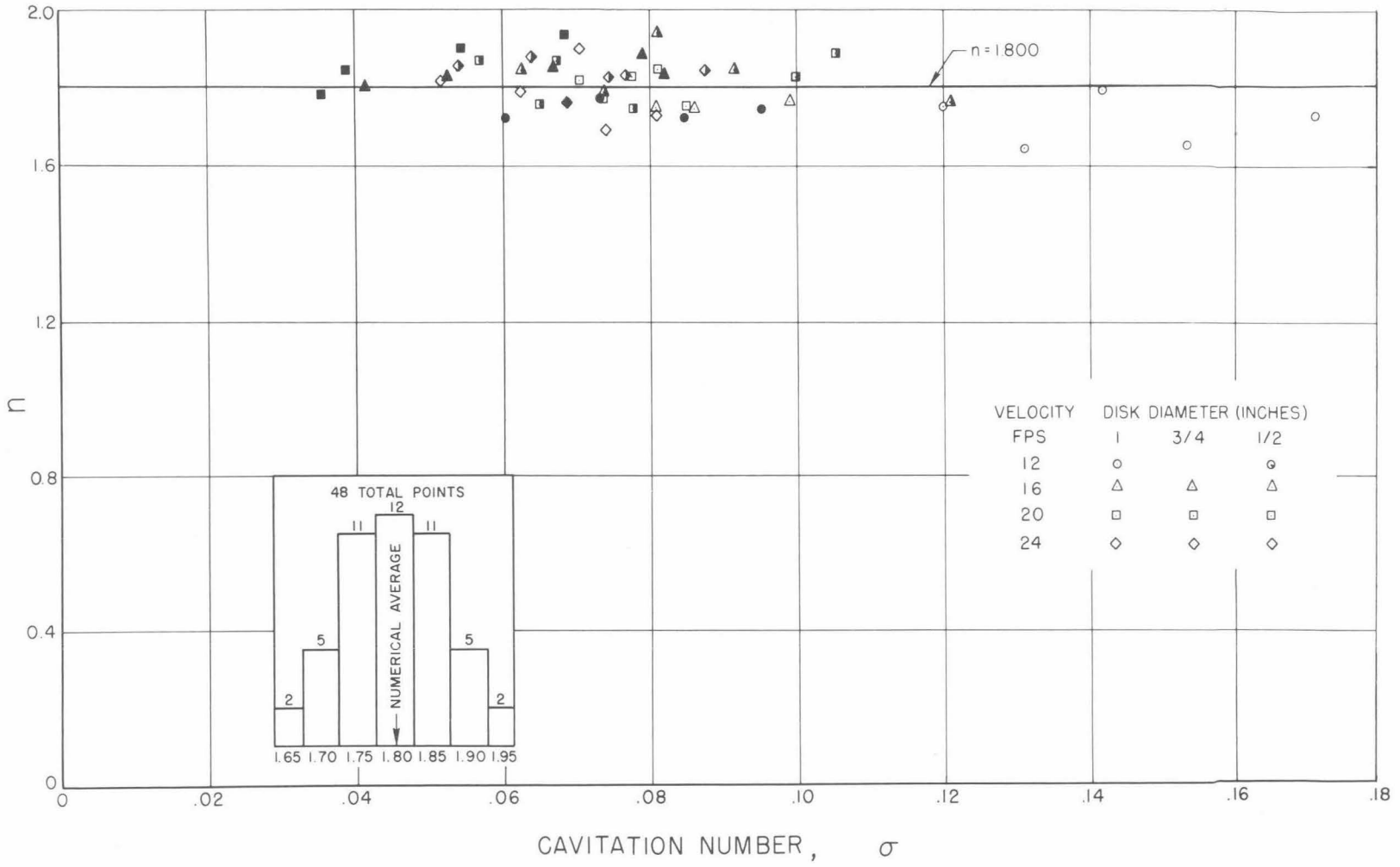

Fig. 15. n as a function of cavitation number ($\alpha = 0^{o}$)

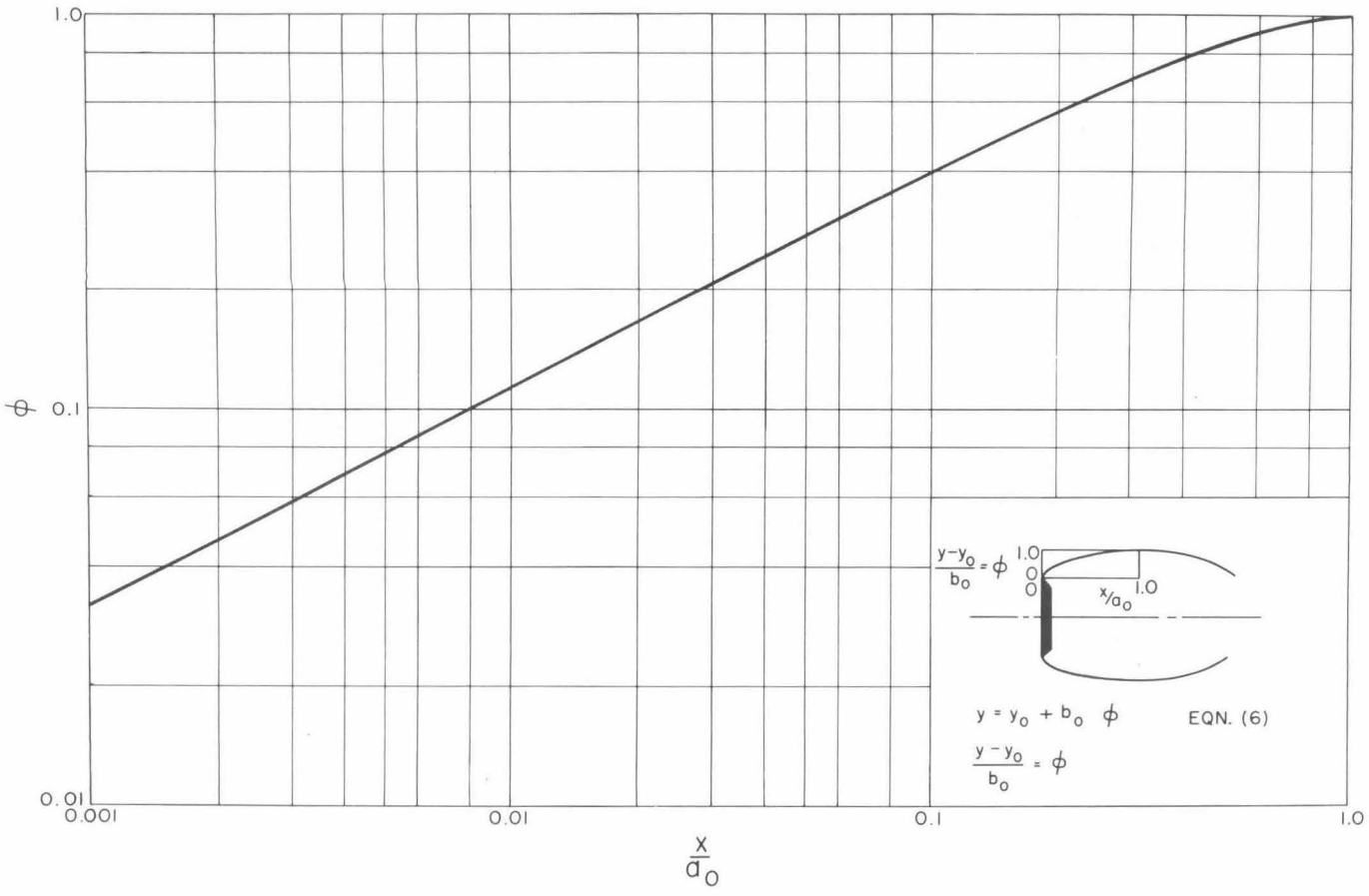

x/a_o	φ	x/a_o	φ	x/a_o	φ
0.000	0.000	.10	.397	.60	.908
.001	.032	.15	.491	.65	.930
.005	.076	.20	.567	.70	.949
.01	.114	.25	.632	.75	.964
.02	.166	.30	.688	.80	.978
.03	.208	.35	.737	.85	.987
.04	.243	.40	.780	.90	.994
.05	.274	.45	.819	.95	.999
.06	.304	.50	.852	1.00	1.000
.08	.353	.55	.882		

Fig. 16. $\phi = \left[1 - \left(\frac{x}{a_o} - 1\right)^2\right]^{\frac{1}{1.800}}$ as a function of x/a_o

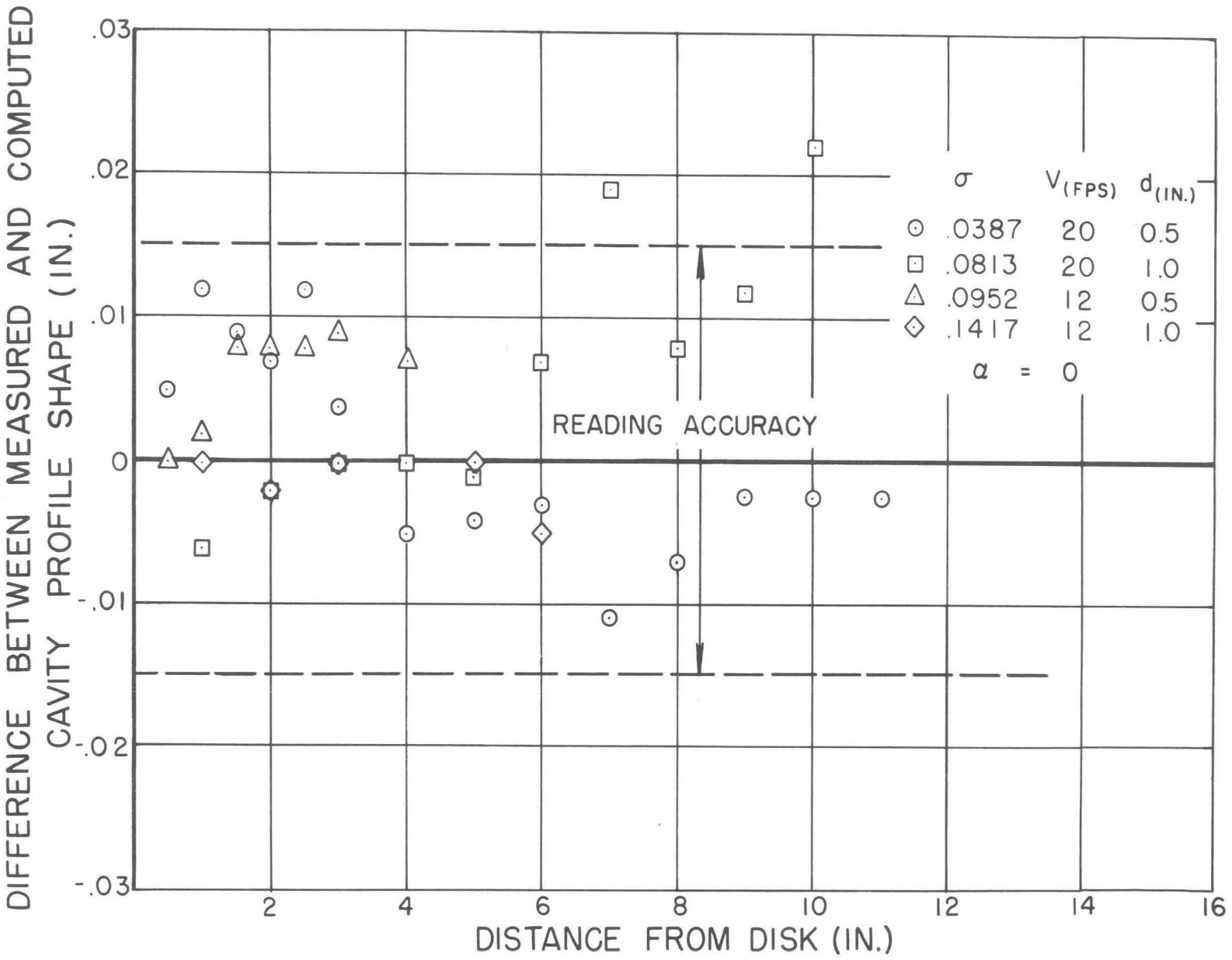

Fig. 17. Difference between measured and computed cavity shapes ($\alpha = 0^{o}$)

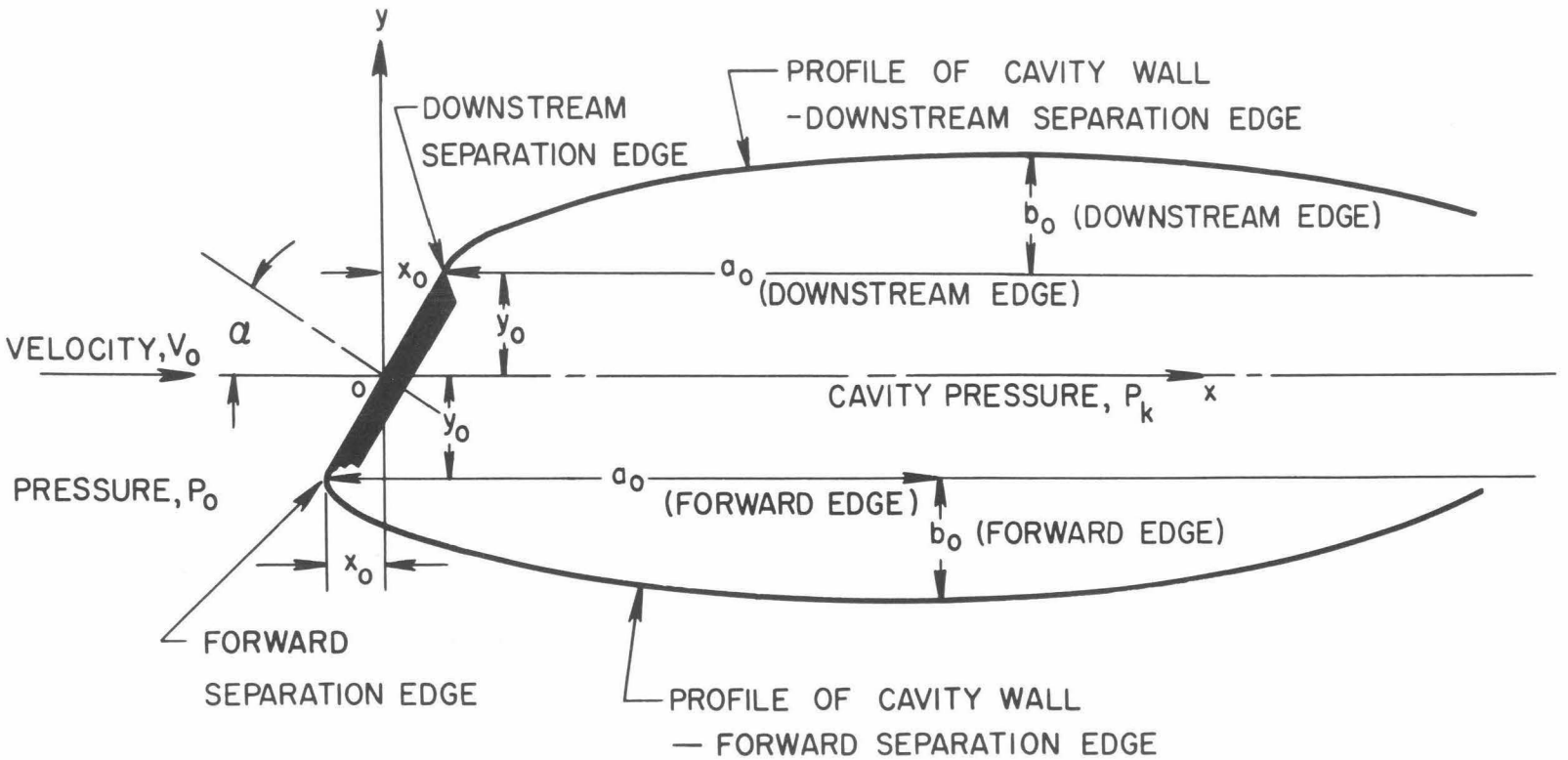

Fig. 18. Analytic description of cavity profile at angle of attack

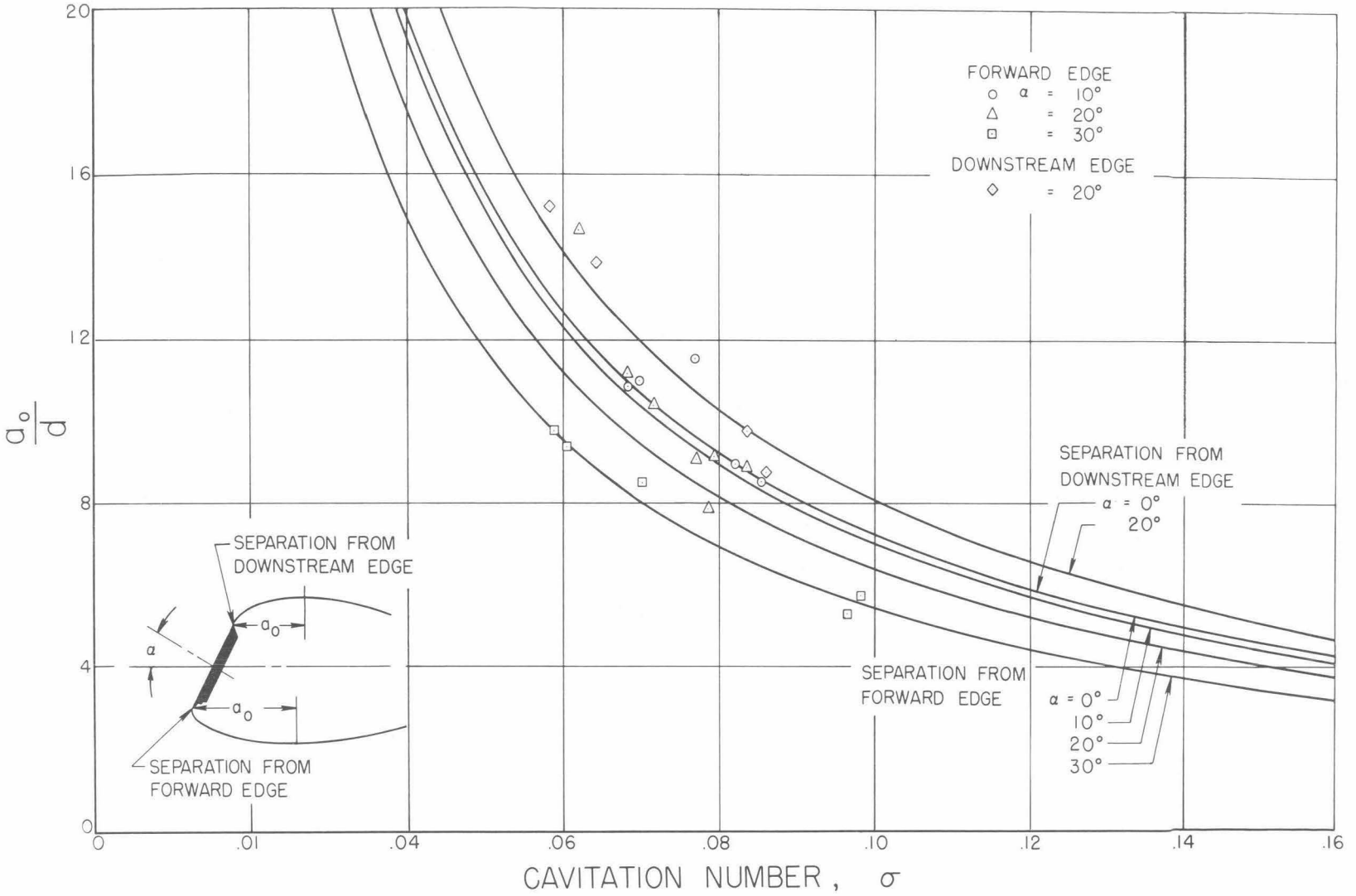

Fig. 19. a_o/d as a function of cavitation number (α up to 30°)

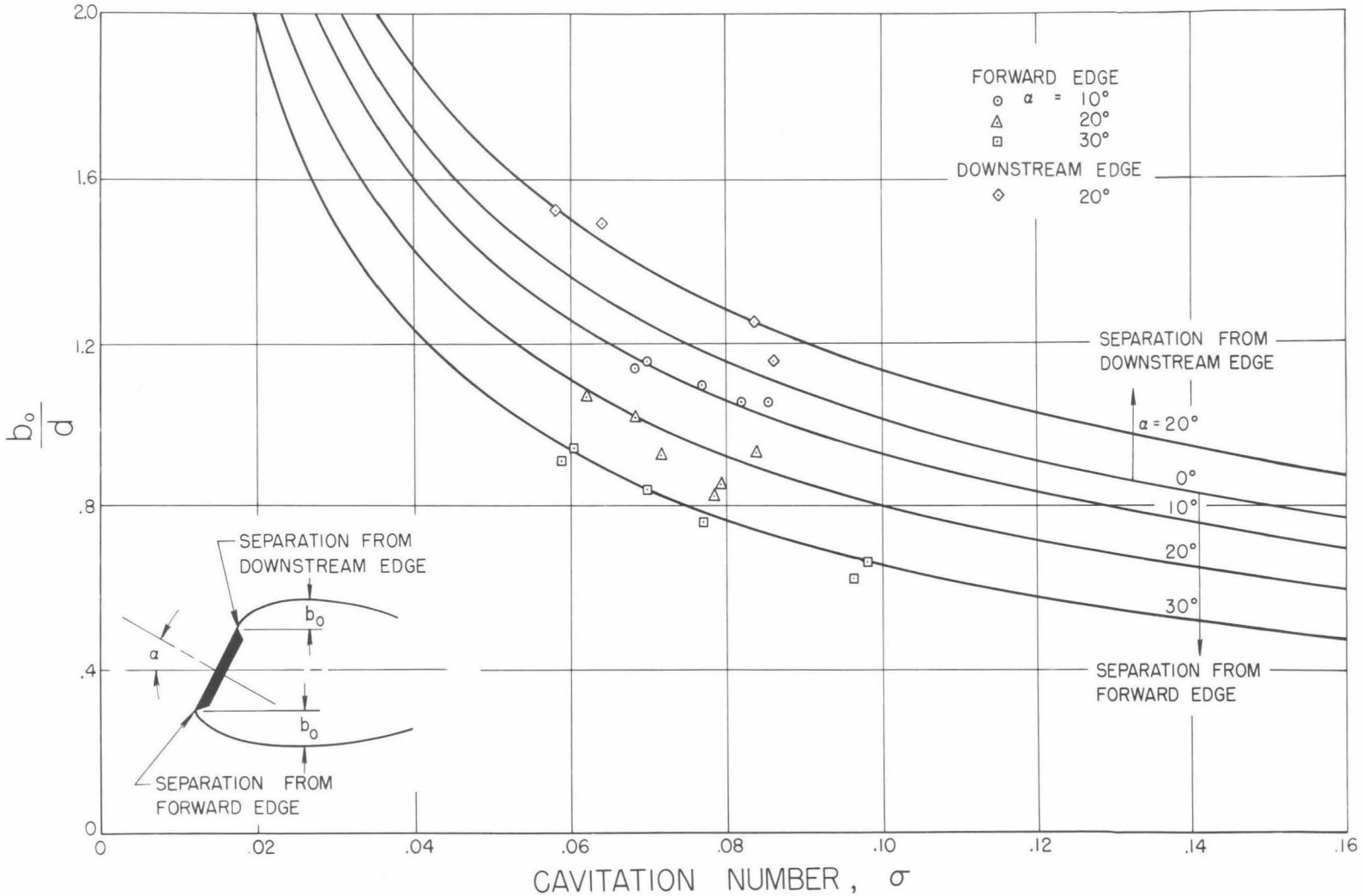

Fig. 20. b_o/d as a function of cavitation number (α up to 30^o)

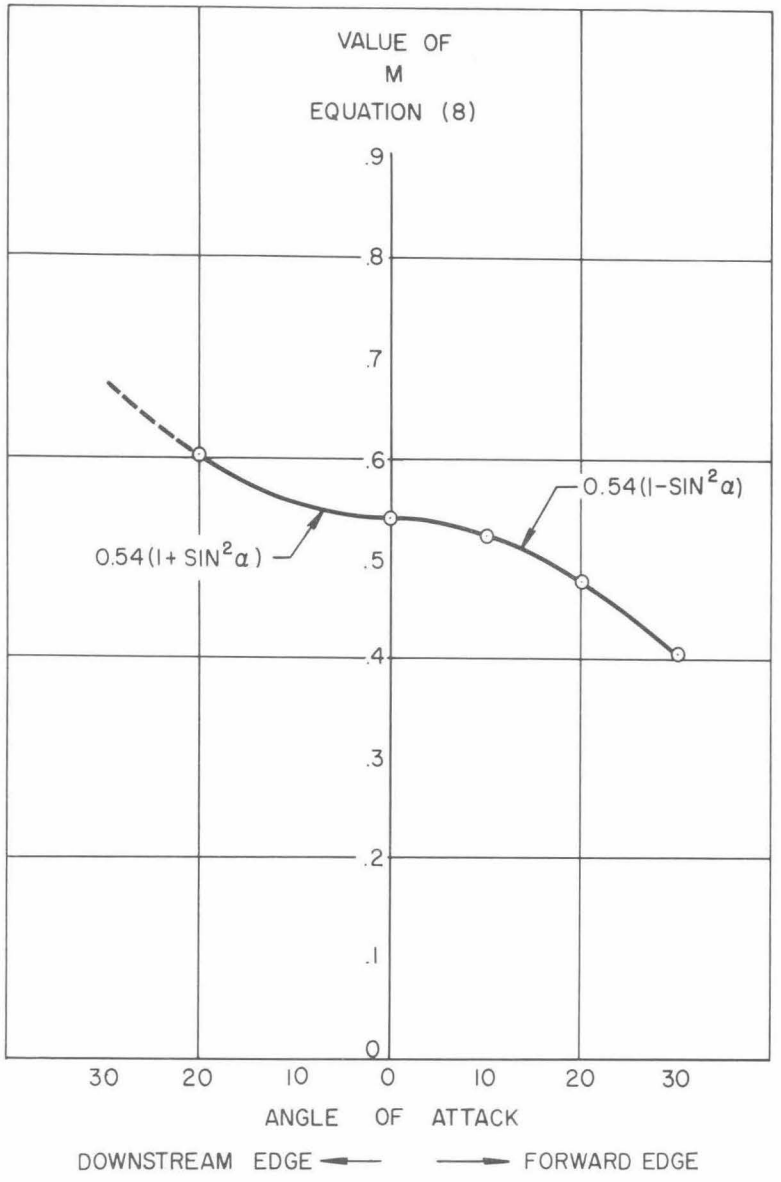

Fig. 21. Empirical function M for equation (8)

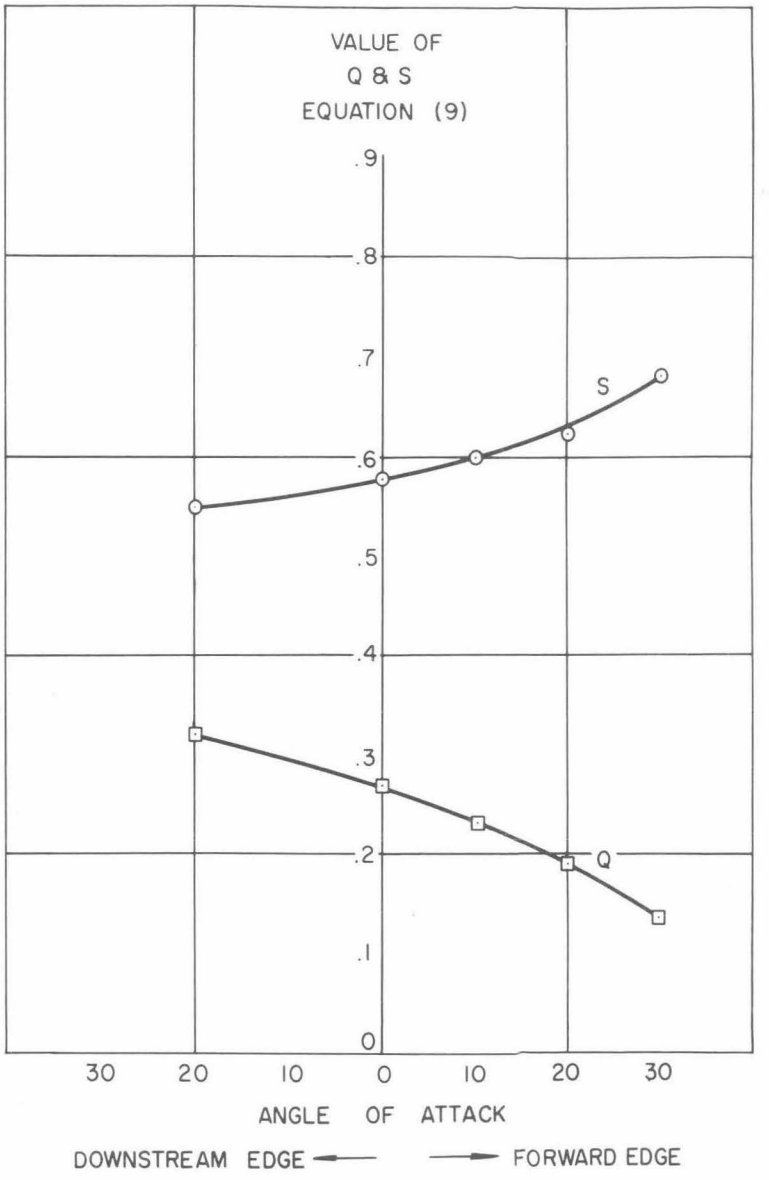

Fig. 22. Empirical functions Q and S for equation (9)

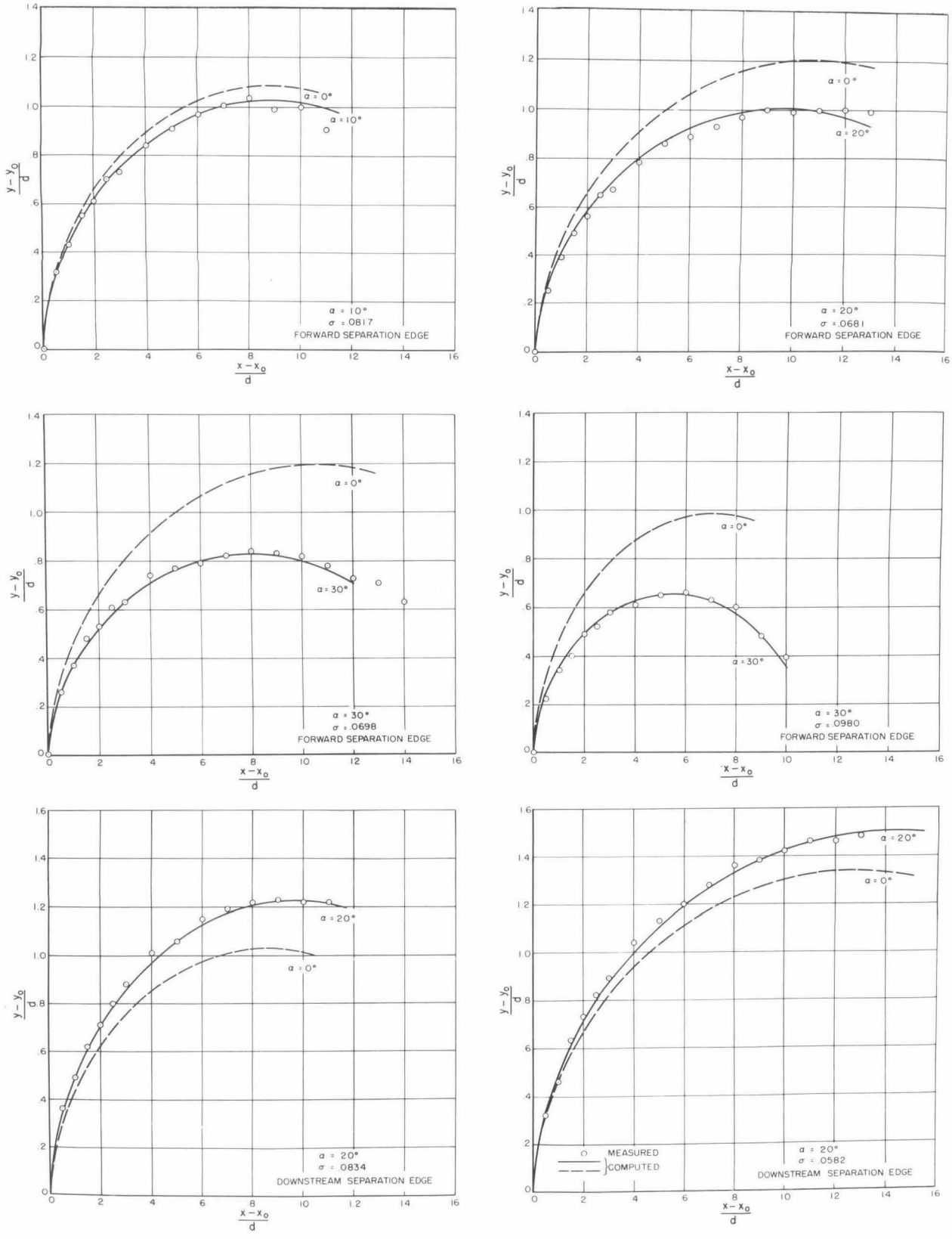

Fig. 23. Comparison of computed and measured cavity shapes at angles of attack

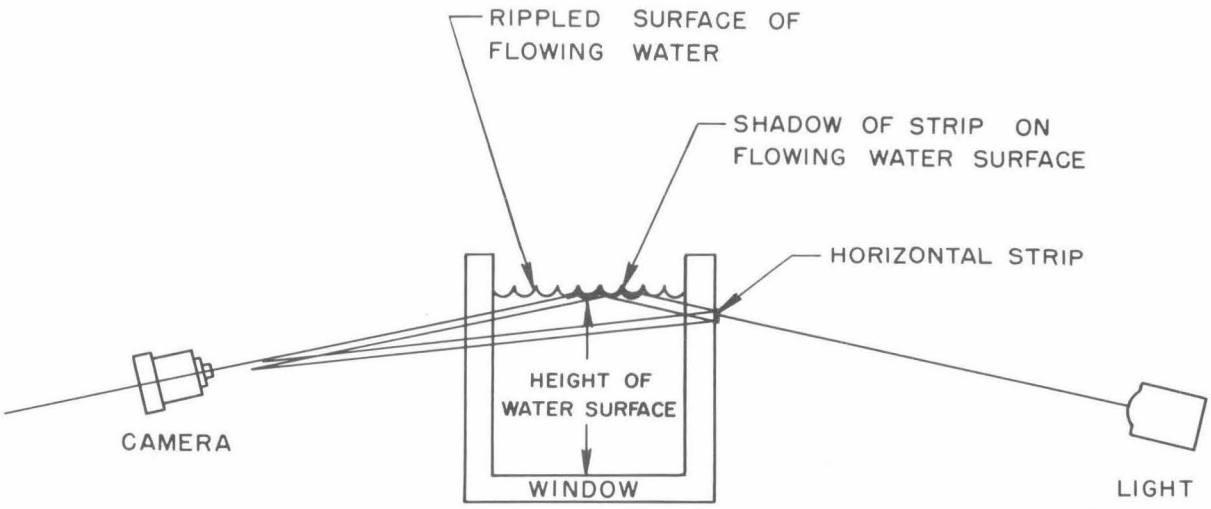

Fig. 24. Techniques for calibrating the free water surface

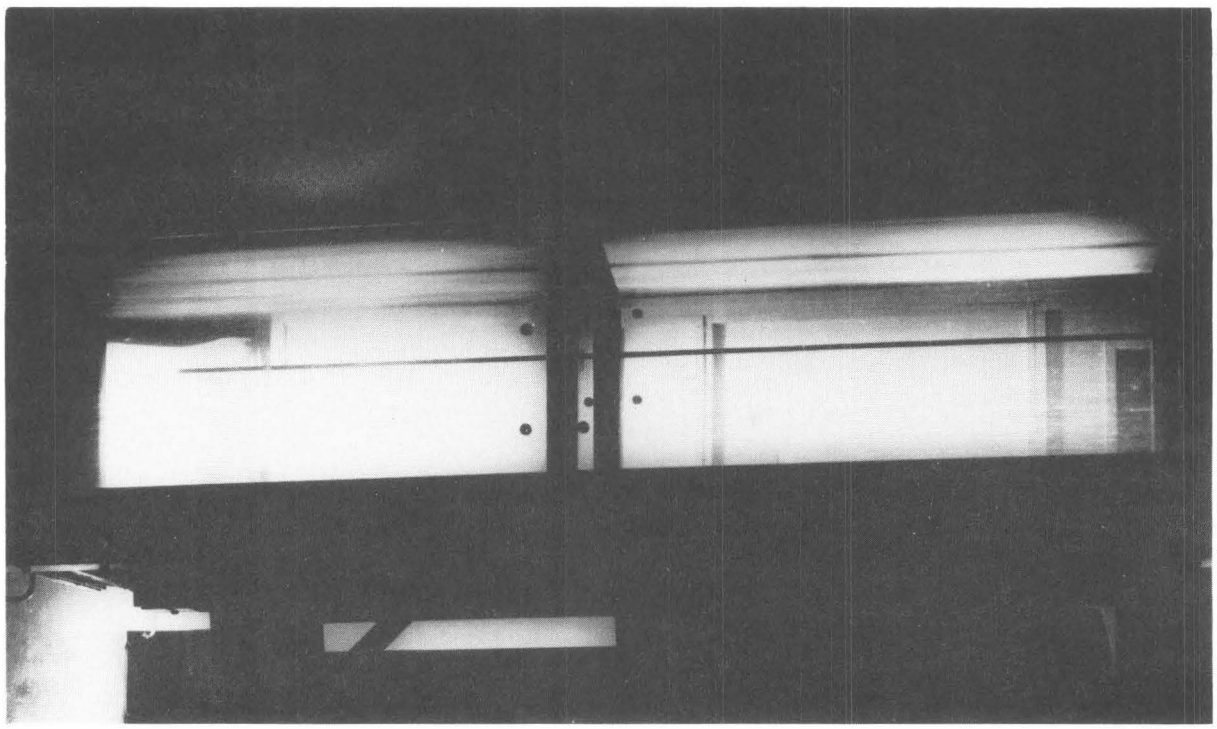

Fig. 25. Typical flow calibration photograph

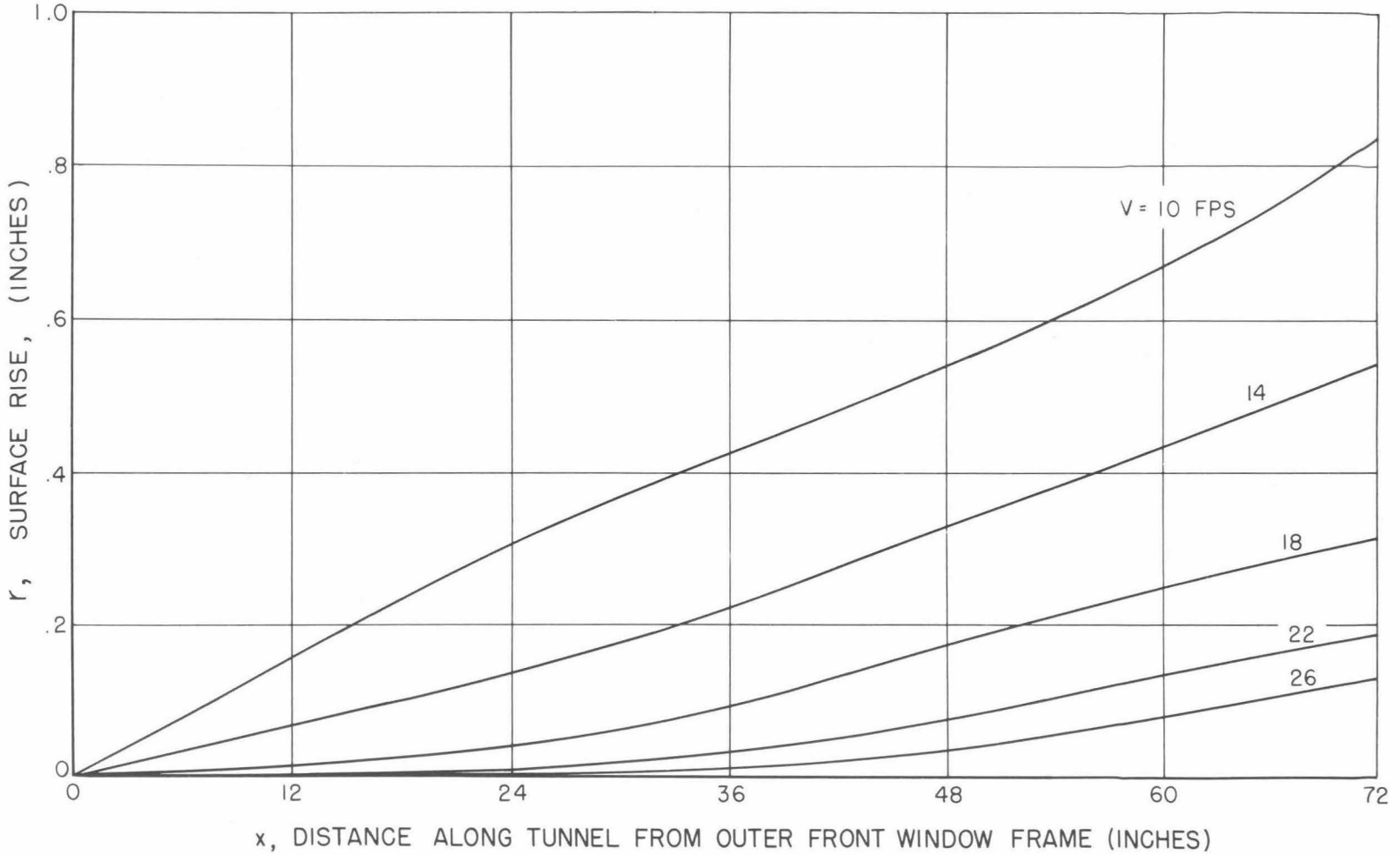

Fig. 26. Rise of free water surface as a function of distance along tunnel for several free stream velocities

DISTRIBUTION LIST

Copy No.	
1-4	Chief, Bureau of Ordnance, Navy Dept., Washington 25, D. C. Attn: Code ReO-3
5-8	Chief, Bureau of Ordnance, Navy Dept., Washington 25, D. C. Attn: Code ReU
9-10	Chief, Bureau of Ordnance, Navy Dept., Washington 25, D. C. Attn: Code Ad3
11-13	Chief, Bureau of Aeronautics, Navy Dept., Washington 25, D. C.
14-18	Chief, Bureau of Ships, Navy Dept., Washington 25, D. C.
19-21	Chief, Office of Naval Research, Navy Dept., Washington 25, D. C. Attn: Code 438
22	Commanding Officer, Office of Naval Research Branch Office, 1030 East Green Street, Pasadena 1, California
23-24	Commanding Officer and Director, David Taylor Model Basin, Washington 7, D. C.
25-26	Commanding Officer, U. S. Naval Underwater Ordnance Station, Newport, Rhode Island
27-28	Commander, U. S. Naval Ordnance Laboratory, White Oak, Silver Spring, Maryland
29-30	Commander, U. S. Naval Ordnance Test Station, Pasadena, California
31	Commander, U. S. Naval Ordnance Test Station, China Lake, California
32	Director, Experimental Towing Tank, Stevens Institute of Technology, via: Bureau of Aeronautics Representative c/o Bendix Aviation Corp., Eclipse-Pioneer Division, Teterboro, New Jersey
33	Director, Ordnance Research Laboratory, Pennsylvania State University, University Park, Pennsylvania
34	Alden Hydraulic Laboratory, Worcester Polytechnic Institute, Worcester, Mass., via: Inspector of Naval Material, 495 Summer Street, Boston 10, Mass.
35-36	Librarian, U. S. Naval Postgraduate School, Monterey, Calif.

DISTRIBUTION LIST (cont'd)

Copy No.	
37-46	British Joint Services Mission, Navy Staff, via: Chief, Bureau of Ordnance, Navy Dept., Washington 25, D. C., Attn: Code Ad8
47-49	Commander, U. S. Naval Proving Ground, Dahlgren, Virginia
50-51	National Advisory Committee for Aeronautics, Langley Memorial Aeronautical Laboratory, Langley Field, Virginia
52	National Advisory Committee for Aeronautics, Lewis Flight Propulsion Lab., Cleveland Airport, Cleveland, Ohio
53	Director, National Advisory Committee for Aeronautics, 1512 H Street, N. W., Washington 25, D. C.
54	Director, National Advisory Committee for Aeronautics, Ames Laboratory, Moffett Field, California
55-56	Commander, Air Research and Development Command, Post Office Box 1395, Baltimore 3, Maryland
57	ASTIA Reference Center, Technical Information Division, Library of Congress, Washington 25, D. C.
58-63	Director, Armed Services Technical Information Agency, Documents Service Center, Knott Building, Dayton 2, Ohio. Attn: DSC-SA

BIBLIOGRAPHY

(For Report No. E-73.4, dated September 1957,
"Cavity Shapes for Circular Disks at Angles of Attack"
by R.L.Waid
Hydrodynamics Laboratory, California Institute of Technology
Pasadena, California)

1. Reichardt, H., "The Laws of Cavitation Bubbles at Axially Symmetrical Bodies in a Flow", Ministry of Aircraft Production, Reports and Translations, No. 766, August 1946, ONR.

2. Self, M.W., Ripken, J.F., "Steady-State Cavity Studies in a Free Jet Water Tunnel", St. Anthony Falls Hydraulic Laboratory, University of Minnesota, Report No. 47.

3. Eisenberg, P., and Pond, H.L., "Water Tunnel Investigations of Steady State Cavities", David Taylor Model Basin, Report No. 668, October 1948.

4. Eisenberg, P., "On the Mechanism and Prevention of Cavitation", David Taylor Model Basin, Report No. 712, July 1950.

5. Knapp, R.T., Levy, J., O'Neill, J.P., and Brown, F.B., "The Hydrodynamics Laboratory of the California Institute of Technology," Trans. ASME, Vol. 70, No. 5, July 1948, pp.437-457.

6. Swanson, W.M., and O'Neill, J.P., "The Stability of an Air-Maintained Cavity Behind a Stationary Object in Flowing Water", California Institute of Technology, Hydrodynamics Laboratory Memo. Report No. M-24.3, September 1951.

7. O'Neill, J.P., "Flow Around Bodies with Attached Open Cavities", California Institute of Technology, Hydrodynamics Laboratory Report No. E-24.7, December 1954.

8. Kiceniuk, T., "An Experimental Study of the Hydrodynamic Forces Acting on a Family of Cavity-Producing Conical Bodies of Revolution Inclined to the Flow", California Institute of Technology Hydrodynamics Laboratory Report No. E-12.17, June 1954.